



The potential of TEMPO-oxidized cellulose nanofibrils as rheology modifiers in food systems

Ragnhild Aaen · Sébastien Simon · Fredrik Wernersson Brodin · Kristin Syverud 

Received: 27 December 2018 / Accepted: 22 April 2019 / Published online: 2 May 2019
© Springer Nature B.V. 2019

Abstract Cellulose nanofibrils (CNFs) have been proposed for use in low-fat food products due to their availability and excellent viscosifying and gel forming abilities. As the CNFs are negatively charged, the presence of other components in foods, such as electrolytes and food additives such as xanthan gum is likely to affect their rheological properties. Hence, the study of these interactions can contribute valuable information of the suitability of CNFs as rheology modifiers and fat replacers. Rheological measurements on aqueous dispersions of TEMPO-oxidized CNFs were performed with variations in concentration of CNFs, concentration of electrolytes and with

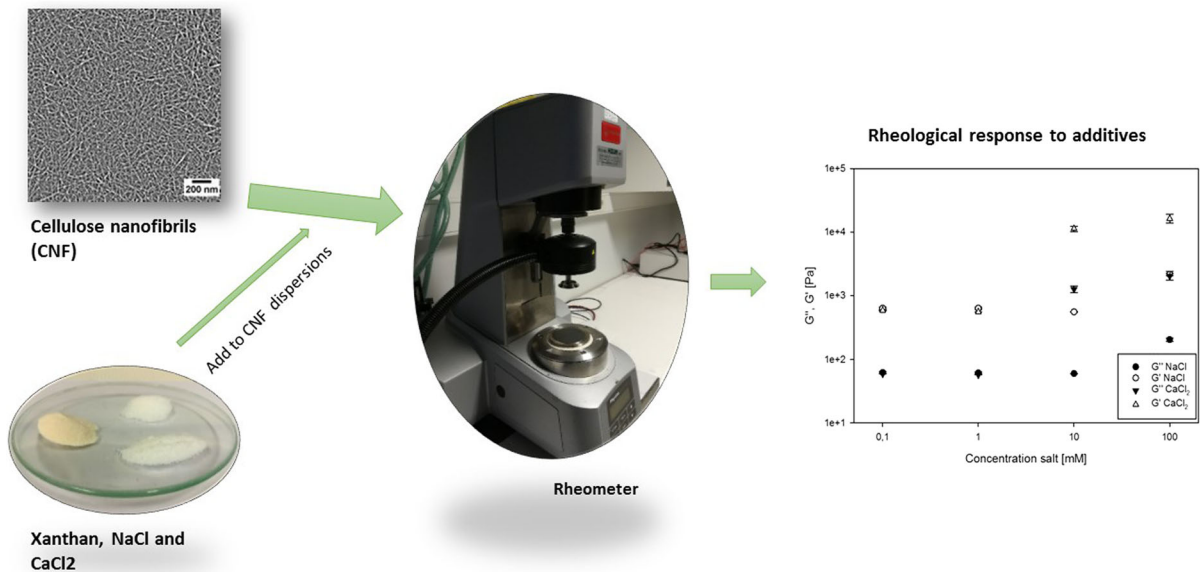
varying CNF/xanthan ratios. UV–Vis Spectroscopy was used to evaluate the onset of CNF flocculation/aggregation in the presence of electrolytes. The CNF dispersions followed a power-law dependency for viscosity and moduli on CNF concentration. Low electrolyte additions strengthened the CNF network by allowing for stronger interactions, while higher additions led to fibril aggregation, and loss of viscosity, especially under shear. The CNF/xanthan ratio, as well as the presence of electrolytes were shown to be key factors in determining whether the viscosity and storage modulus of CNF dispersions increased or decreased when xanthan was added.

Electronic supplementary material The online version of this article (<https://doi.org/10.1007/s10570-019-02448-3>) contains supplementary material, which is available to authorized users.

R. Aaen · S. Simon · K. Syverud (✉)
Ugelstad Laboratory, Department of Chemical Engineering, Norwegian University of Science and Technology, 7491 Trondheim, Norway
e-mail: kristin.syverud@rise-pfi.no

F. Wernersson Brodin · K. Syverud
RISE PFI, 7491 Trondheim, Norway

Graphical abstract



Keywords Nanocellulose · Cellulose nanofibrils (CNFs) · Rheology · Food additives · TEMPO-mediated oxidation · Ionic strength

Introduction

Obesity is a growing health problem attributed to diets dominated by an excess of energy-dense foods with a high content of fat and sugar, and carries with it an increased risk of many diseases such as diabetes 2 and cardiovascular diseases (Isomaa et al. 2001; James et al. 2004; Van Gaal et al. 2006). The Dietary Guidelines for several countries state that the intake of especially saturated fats should be reduced, and that dairy products should be consumed mainly in fat-free or low-fat forms (Food Standards Agency 2010; U.S. Department of Health and Human Services and U.S. Department of Agriculture 2015). With the increased focus on the fat content of food, many food companies strive to develop low fat and no fat products for their consumers. Removing fat from a food product can however cause the loss of qualities such as a desirable appearance, flavor, aroma, texture and mouthfeel, properties that must then be obtained by the addition of so called fat replacers (Lucca and

Tepper 1994; Roller and Jones 1996). Fat replacers can generally be protein-, carbohydrate- or fat-based, where the different types will give the product varying properties (González-Tomás et al. 2007; Lucca and Tepper 1994; Sandoval-Castilla et al. 2004). The carbohydrate-based fat replacers are generally used for structuring the water phase, increasing the viscosity and contribute to a mouthfeel similar to that of fat (Lucca and Tepper 1994; Mudgil and Barak 2013). A combination of several fat replacers will often be necessary to obtain the desired properties in low fat foods (Lucca and Tepper 1994).

Cellulose, a material consisting of glucose chains, is known as the most abundant biopolymer on earth, and is the main constituent of the cell walls of higher plants (Payen 1838; Purves 1954; Saxena and Brown Jr 2005). Structures known as elementary fibrils, with diameters of approximately 3.5 nm, are constituted of glucan chains associated through van der Waals forces and hydrogen bonding (Cousins and Brown 1997; Gardner and Blackwell 1974; Heyn 1969). These fibrils can be extracted from cellulosic pulps by mechanical treatment, often used in combination with some kind of pretreatment of the pulp to reduce the energy requirements (Herrick et al. 1983; Pääkkö et al. 2007; Saito and Isogai 2004; Turbak et al. 1983). One kind of pretreatment is oxidation of the

primary hydroxyl groups on the cellulose fibrils with sodium hypochlorite in a reaction catalyzed by 2,2,6,6-tetramethylpiperidine-1-oxyl radical (TEMPO) (Saito and Isogai 2004, 2006). The oxidation introduces charges into the fibers through carboxylate groups, which contributes to an easier and less energy demanding disintegration of the fibers into nanofibrils. The wood cellulose nanofibrils (CNFs) produced by this method can have widths in the range of a few nanometers and lengths up to a few microns, giving very viscous suspensions even with a very low solid fraction (Saito et al. 2006, 2007).

CNF suspensions, both from pretreated and non-pretreated fibrils, exhibit a shear thinning behavior, and shear rate- viscosity curves show a yield stress and a hysteresis loop at low shear rates above a certain concentration of CNFs (Iotti et al. 2011; Lasseguette et al. 2008; Naderi et al. 2014a; Pääkkö et al. 2007). The critical overlap concentration for CNF systems, where the suspension shifts from a Newtonian flow to a non-Newtonian flow, has been found in the region 0.2–0.3 wt% for a low shear rate around 0.1 s^{-1} (Lasseguette et al. 2008; Lowys et al. 2001; Tatsumi et al. 2002). Above this concentration the formation of a network begins due to the entanglement of the fibrils (Lowys et al. 2001). All the rheological properties of CNF systems are heavily dependent on the concentration of CNFs in the suspension, with a power law dependency between both the storage modulus and the viscosity on the concentration, as long as the concentration ranges well above the critical overlap concentration (Naderi et al. 2014b; Pääkkö et al. 2007). For the storage modulus, G' , the dependency on the CNF concentration can be represented by a power law on the form given in Eq. 1.

$$G' = kc^\alpha \quad (1)$$

where G' is the storage modulus, k and α are constants, and c is the concentration of CNFs.

The value of α has been reported to be 2.25 for acid hydrolysed and bacterial cellulose, 2.4 for carboxymethylated CNFs, 2.25 and 2.58 for mechanically treated CNFs and 3 for enzymatically treated CNFs (Agoda-Tandjawa et al. 2010; Naderi et al. 2014b; Pääkkö et al. 2007; Tatsumi et al. 2002). Similarly, the viscosity of suspensions fitted to a power law on the form given in Eq. 2 have given

values for β between 2 for a carboxymethylated sample to 6 for a TEMPO-oxidized sample at a shear rate of 0.1 s^{-1} (Lasseguette et al. 2008; Naderi et al. 2014b). Great variations with shear rate can be found for the same sample, as shown by Lasseguette et al. (2008), where the value of β varied between 2 for a shear rate of 100 s^{-1} and 6 for a shear rate of 0.1 s^{-1} .

$$\eta = k * c^\beta \quad (2)$$

where η is the viscosity, k^* and β are constants, and c is the concentration of CNF.

In a food system, electrolytes in some form will usually be present, and the rheological response to addition of electrolytes could determine the usability of CNFs as fat replacers in these systems. Based on the Derjaguin–Landau–Verwey–Overbeek (DLVO) theory of colloid stability CNF dispersions will stay stable as long as the electrostatic repulsion between the fibrils is stronger than the attractive van der Waals forces between them (Derjaguin and Landau 1941; Saarikoski et al. 2012; Verwey and Overbeek 1948). The addition of electrolytes changes the balance between these forces, and as counter-ions such as Na^+ or Ca^{2+} gather close to the charged fibril surface, they contribute to a lower surface charge as well as an electrostatic screening of the negative charges (Fall et al. 2011; Saarikoski et al. 2012). The closer contact between the fibrils allows for a strengthening of the fibril contact points resulting in a stronger network, leading to higher viscosity and storage modulus, G' , for the CNF dispersion (Agoda-Tandjawa et al. 2010; Dong et al. 2013; Lowys et al. 2001; Saarikoski et al. 2012). Metal-carboxylate binding can in addition allow for gelation of carboxylated CNF dispersions by inter- and intrafibrillar crosslinking when divalent and trivalent cations are present (Aarstad et al. 2017; Dong et al. 2013). As the concentration of counter-ions increases, the screening of negative charges can however reduce the electrostatic repulsion enough to cause a collapse of the CNF network, leaving permanent fibril aggregates surrounded by dispersion medium, causing lower viscosity and moduli (Naderi and Lindström 2014; Saarikoski et al. 2012).

The perceived textural properties of food, such as the property of creaminess and thickness can, to some degree, be predicted by looking at the rheological

data of the food (Cheung et al. 2002; Jellema et al. 2005; Torres et al. 2011).

In this study, we have investigated fundamental rheological properties of TEMPO-oxidized CNFs, both in pure water and in electrolyte solutions, to evaluate their usability as fat replacers in foodstuff. We have also studied their rheological interaction with the commonly used food additive xanthan gum. The study is also relevant for other fluids in which CNF could be used for rheology control, e.g. inks for 3D printing (Heggset et al. 2019) and drilling fluids (Heggset et al. 2017).

Materials and methods

Materials

The studied CNFs were prepared at RISE PFI, Norway, from a dissolving pulp (Borregaard, Sarpsborg, Norway). The pulp was subjected to TEMPO-mediated oxidation as described by Saito and Isogai (2004). In short, 110 g cellulose was suspended in 8.25 L of deionized water containing 1.375 g TEMPO and 13.75 g sodium bromide before sodium hypochlorite was added to start the reaction. The start concentration of sodium hypochlorite in the reaction mixture was set at 1.7, 2.8 or 3.5 mmol NaClO per gram of cellulose, giving CNF oxidized to three different levels. The pH was kept at 10.5 during the reaction by adding 0.5 M sodium hydroxide. When the pH stayed constant without addition of more sodium hydroxide, the pH was adjusted to 7 by use of 0.5 M hydrochloric acid. The samples were washed thoroughly with deionized water on a Büchner funnel until the conductivity was less than 5 $\mu\text{S}/\text{cm}$, and named as CNF-LC for low charge, CNF-MC for medium charge and CNF-HC for high charge. The charge densities of the three samples were analyzed by conductometric titration before homogenization, as described by Saito and Isogai (2006).

The pre-treated samples, with a dry content of about 1% were homogenized using a high-pressure homogenizer (Rannie 15 type 12.56 \times homogenizer APV, SPX Flow Technology, Silkeborg, Denmark) at two passes, the first at 600 bar, and the second at 1000 bar.

Calcium chloride dihydrate, 2,2,6,6-tetramethylpiperidine-1-oxyl radical and xanthan gum

were obtained from Sigma-Aldrich Co. (Steinheim, Germany). Sodium chloride and sodium bromide was purchased from Merck (Darmstadt, Germany). The sodium hypochlorite was obtained from Carl Roth (Karlsruhe, Germany). All chemicals were of laboratory grade, and used without further purification. The ultrapure Milli-Q water used in the experiments was dispensed through a 0.22 μm Millipore filter and had a resistivity of 18.2 $\text{M}\Omega\ \text{m}$ at 25 $^{\circ}\text{C}$ (Merck Millipore, Darmstadt, Germany).

Preparation of samples

The CNF samples shown in Table S1 in Supplementary were prepared from start concentrations of about 1.1 wt% CNFs and 5 M stock solutions of NaCl and CaCl_2 . All samples were stirred with a Eurostar Digital stirrer (IKA, Staufen Germany) equipped with a four bladed propeller for 10 min at 2000 rpm after addition of all the components. The samples were stored at 4 $^{\circ}\text{C}$, for at least 2 days before the measurements were performed. The focus in this study was on the CNF-MC sample, but the CNF-LC and CNF-HC were included in some of the experiments to obtain some information about the effect of charge density, especially on flocculation or aggregation.

Dry xanthan gum was dissolved in water by stirring with a Eurostar Digital stirrer (IKA, Staufen Germany) equipped with a four bladed propeller for 1 h at 2000 rpm to give a 1.11 wt% solution. The xanthan solution or/and the CNF-MC was mixed with either water or salt solution at 2000 rpm for 10 min to give the samples shown in Table S2. In this experiment, we used NaCl for the salt solution, while CaCl_2 may be used in a later study.

Atomic force microscopy (AFM)

Images of the CNF samples were acquired by atomic force microscopy (AFM), using a Bruker Multimode V AFM with a Nanoscope V Controller (Veeco Instruments Inc., Santa Barbara, CA, USA). A drop of aqueous CNF dispersion with concentration 0.01 wt% was placed on freshly cleaved 10 mm mica (Agar Scientific Ltd. Essex, UK) and dried using compressed N_2 gas. The operation mode used was quantitative nanomechanical mapping (QNM) with automated settings, and the images were

acquired using the Scan Asyst mode in air at ambient temperature, with a nominal spring constant of 0.4 Nm^{-1} and resonance frequency 70 kHz. Silicon nitride AFM tips, SA-air, were provided by Bruker AFM Probes (Bruker Nano Inc., Camarillo, CA, USA).

Ultraviolet–visible (UV–Vis) spectroscopy

Transmittance have been previously been used as an indirect way of evaluating the degree of aggregation or flocculation of CNFs, as the aggregation leads to increased light scattering (Chen et al. 2011; Fukuzumi et al. 2014). The change in transmittance of CNF dispersions of different charge densities upon addition of electrolytes was investigated using a UV–Vis Spectrophotometer (UV-2401PC, Shimadzu, Tokyo, Japan). The addition of electrolytes is expected to reduce the electrostatic repulsion between the fibrils and eventually lead to aggregation. As the transmittance decreases with an increasing particle size, UV–Vis spectroscopy can give an indication of the degree of aggregation in the samples as electrolyte is added. Series of CNF dispersions containing between 0.1 and 100 mM sodium chloride or calcium chloride were prepared according to the procedure described in “[Preparation of samples](#)” section, and the transmittance was measured for wavelengths 300–800 nm using a cell path length of 1 cm and a slit width of 2.0 nm. At least two parallels were recorded for each sample. The average transmittance at 500 nm for each sample was compared to that of a 0.11 wt% CNF sample containing no electrolytes.

Rheological measurements

The rheological properties of the CNF-MC dispersions and xanthan solutions were evaluated using a Physica MCR 301 rheometer (Anton Paar GmbH, Graz, Austria) equipped with a cone and plate geometry. The cone and plate had roughened surfaces and a gap size of 0.057 mm. Wall slip, occurring when the disperse phase is displaced away from the solid boundaries in the rheometer, giving a lower apparent viscosity of the suspension, is a known problem for CNF suspensions, especially with electrolytes present (Barnes 1995; Saarikoski et al. 2012). The use of serrated or roughened surfaces in the

rheometer is a way to reduce this wall slip effect (Buscall et al. 1993; Nechyporchuk et al. 2014). The content of the sample bottles was stirred with a spoon before it was loaded unto the plate of the rheometer. All samples were subjected to 1 min of pre-shearing at 100 s^{-1} followed by 2 min of rest before the measurements started.

Rotational measurements

Flow curves were obtained by increasing the shear rate from 0.1 to 1000 s^{-1} over a 10 min period, followed by a down-sweep from 1000 to 0.1 s^{-1} at $20 \text{ }^\circ\text{C}$. The up-sweep and down-sweep were then repeated immediately on the same sample. Two to four parallels were performed for each sample, and the viscosity was measured as a function of the shear rate.

Oscillatory measurements

At least two parallels of strain sweeps were performed on each sample, with the frequency set at 0.01 Hz and the strain ranging between 0.1 and 100% to determine the linear viscoelastic region of the samples. Frequency sweeps were performed in duplicate with the strain set at 1%, which was well within the linear viscoelastic region for all the samples. The frequency was increased from 0.01 to 10 Hz, and the storage and loss moduli were recorded as a function of the frequency at $20 \text{ }^\circ\text{C}$.

Results and discussion

The error bars in Figs. 4, 5, 6, 7, 8, 9 and 10 show the spreading of the data, where the positive and negative bars represent the maximum and minimum value, respectively, obtained for the specific measurement point. For many of the data points the error bars do not reach outside the marker.

Characterization of fibril samples

The charge densities of CNF-LC, CNF-MC and CNF-HC were determined by conductometric titration before homogenization, to be 649 ± 16 , 1068 ± 43 and $1352 \pm 5 \text{ } \mu\text{mol/g}$ respectively. The spreading in the charge density measurements is given as the standard

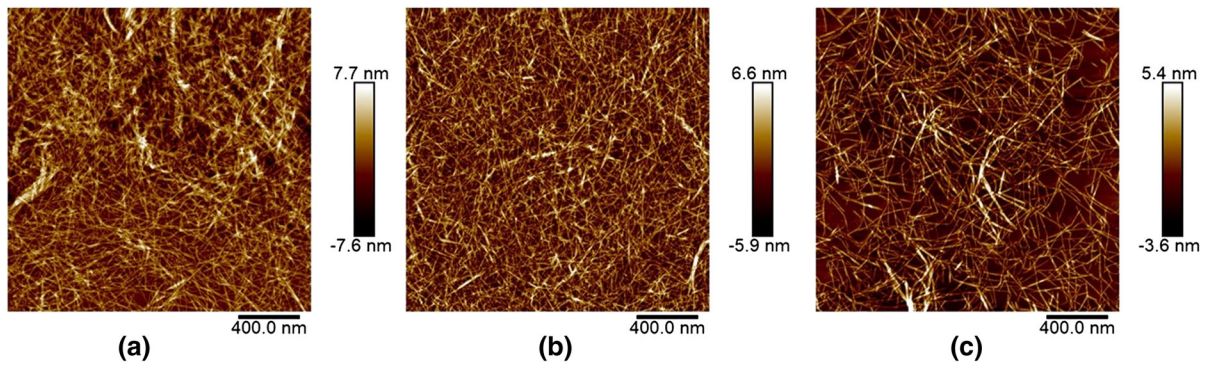


Fig. 1 AFM topographic images of the three CNF samples CNF-LC (a), CNF-MC (b) and CNF-HC (c) after drying on mica. The pictures confirm that all the samples consist of fibrillated material, with a similar morphology for all the samples

error of the mean. AFM images of CNF-LC, CNF-MC and CNF-HC are shown in Fig. 1.

The AFM micrographs of the three different CNFs dried on mica confirm that they consist of fibrillated material, with a similar morphology for all the samples. The fibrils of the sample CNF-LC seems to be somewhat more aggregated than the samples with higher charge densities. The exact dimensions cannot be determined from these pictures, but the aspect ratio, length to width, seems to be quite high for all samples, as should be expected for CNFs obtained by TEMPO-mediated oxidation (Saito et al. 2006, 2007).

Concentration dependency of CNFs on the viscosity and moduli

The viscosity, loss modulus and storage modulus of CNFs prepared by TEMPO-mediated oxidation, with a charge density of $1068 \pm 61 \mu\text{mol/g}$ (CNF-MC), were measured at different concentrations to compare with existing literature. Figure 2 shows the flow curves of CNF-MC at three different concentrations.

The flow curves all show a shear thinning behavior, as shown for other CNF suspensions (Iotti et al. 2011; Lasseguette et al. 2008; Naderi et al. 2014a; Pääkkö et al. 2007). The first down-curve, and both up- and down-curve for the second sweep is superimposed for all the samples, with some signs of thixotropic behavior for the highest concentrations, where the curve from the first up-sweep show a higher viscosity than the remaining curves.

The viscosity at a shear rate of 0.1 s^{-1} from the first up-curve and the last down-curve as a function of

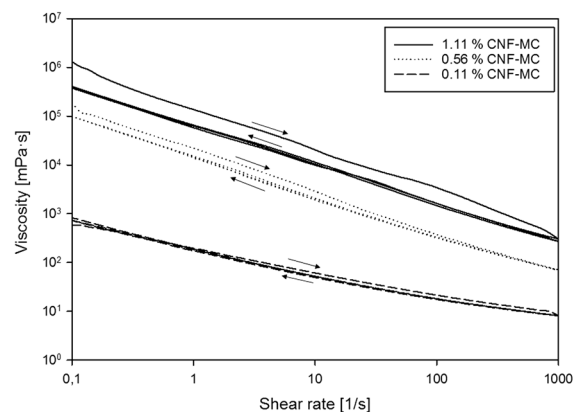


Fig. 2 The viscosity of aqueous CNF dispersions (CNF-MC), at three different concentrations, shown as a function of the shear rate

CNF concentration (Fig. 3) was fitted with a power law on the form of Eq. 2.

The resulting values of β of 3.3 for data from the first up-curve, and 2.6 for the last down-curve indicate that we are in the region where the fibrils overlap. The shear thinning observed in Fig. 2 is attributed to the alignment of the fibrils as well as the “de-overlapping” of CNFs. By comparison, the values taken from a high shear rate of 1000 s^{-1} yields the value 1.4 for β both for the up- and down-sweep. The obtained exponents for low shear values are quite much lower than the value of 6 given by Lasseguette et al. (2008) for another TEMPO-oxidized sample, and closer to the value of 2 found for a carboxymethylated sample prepared by Naderi et al. (2014a, b). The Lasseguette group used a blender with rotating knives rather than high-pressure homogenizer after the pulp was oxidized. Based on

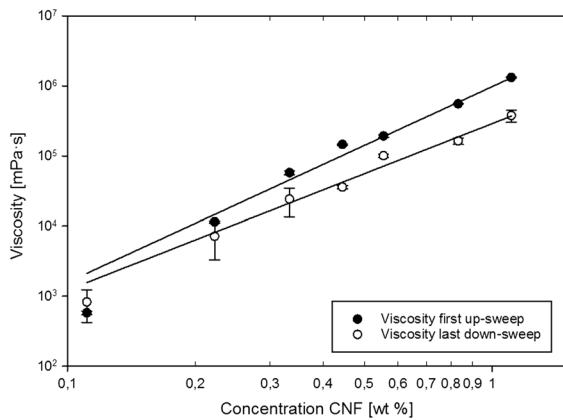


Fig. 3 The viscosity of aqueous CNF dispersions (CNF-MC) at varying concentrations. The results stem from measurements performed in replicates at a shear rate of 0.1 s^{-1} , and the viscosity for the first up-curve and the last down-curve is shown as a function of the CNF concentration. The results are fitted to power law functions, represented by solid lines

the two different preparation methods, the two CNF qualities will differ both in size of the fibrils and in polydispersity, which may explain the large difference in obtained exponent values.

Figure 4 shows the loss and storage moduli as a function of the strain, of CNF-MC at three different concentrations.

Strain sweeps for CNF concentrations 0.11–1.11 wt% show that the higher concentrations yield a larger difference between loss and storage modulus, indicating a more preponderant elastic character

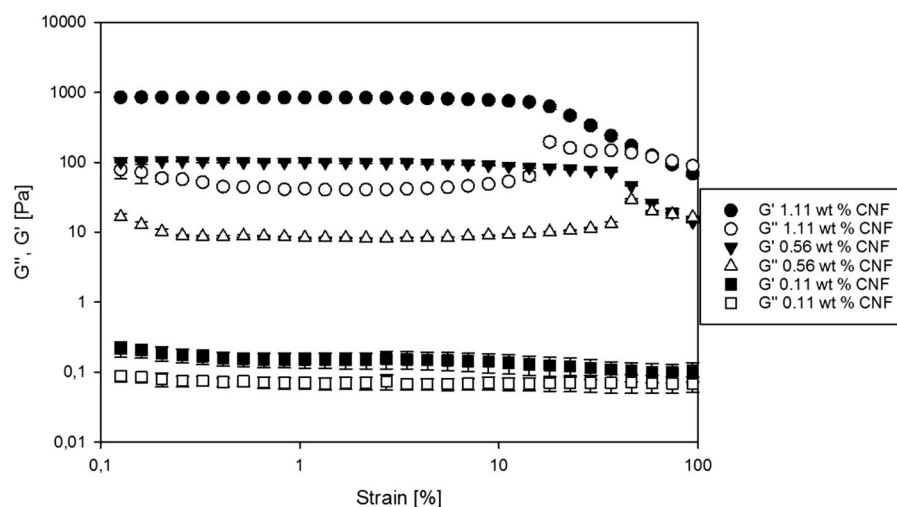


Fig. 4 The loss modulus (G'') and the storage modulus (G') of aqueous CNF-MC dispersions at three different concentrations, shown as a function of the strain

(Herrick et al. 1983). The critical strain, marking the end of the linear viscoelastic region appears high (higher than 10%) and decreases with the concentration (1.11 vs 0.56%). This range corresponds well to results obtained by Naderi and Lindström (2014) and by Jowkarderis and van de Ven (2015).

The moduli both increase with the concentration of CNFs, and a fit to Eq. 1 results in a value for α of 3.6 for the storage modulus, as shown in Fig. 5. This is a slightly higher value than the values ranging between 2.25 and 3 reported by other groups for other types of CNFs (Agoda-Tandjawa et al. 2010; Naderi et al. 2014b; Pääkkö et al. 2007; Tatsumi et al. 2002). The larger response to an increase in concentration can be due to the higher charge density, and thus higher effective fibril volume of our sample, or by morphological factors. The corresponding value from the figure for the loss modulus is 2.7.

Effects of electrolytes on CNF dispersions

In food systems, there is usually electrolytes present, especially in the form of NaCl. As an example, the salt content, given by USDA National Nutrient Database, of some typical foods are 0.7–1.5 g/100 g for mayonnaise, 4.1–9.5 g/100 g for caviar and 0.2–3.5 g/100 g for prepared mashed potatoes (USDA 2018).

The transmittance of electrolyte-containing CNF samples with three different charge densities was

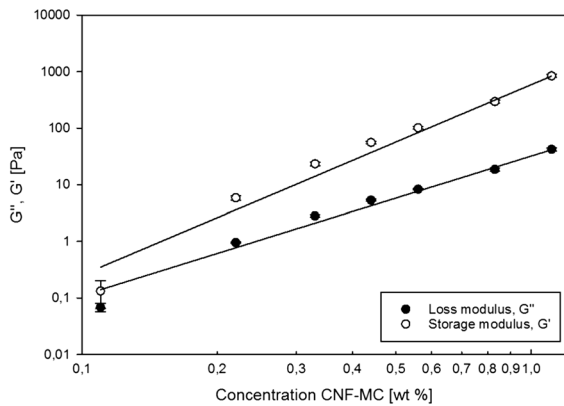


Fig. 5 The loss modulus (G'') and the storage modulus (G') of aqueous CNF-MC dispersions obtained from strain sweeps, at 0.01 Hz and 1% strain, as a function of the CNF concentration. The results are fitted to a power law function for each modulus, represented by solid lines

measured at 300–800 nm to evaluate the onset of fibril aggregation, with the transmittance spectra given in Figure S1–S6 in Supplementary. The transmittance decreases with the degree of CNF aggregation in the dispersion due to an increased light scattering for larger particles. The ratio between measured transmittance at 500 nm and the transmittance of a sample containing no electrolyte is shown as a function of the content of NaCl (a) or CaCl_2 (b) in Fig. 6.

As expected, the transmittance decreases as electrolytes are added to the dispersions, as the screening

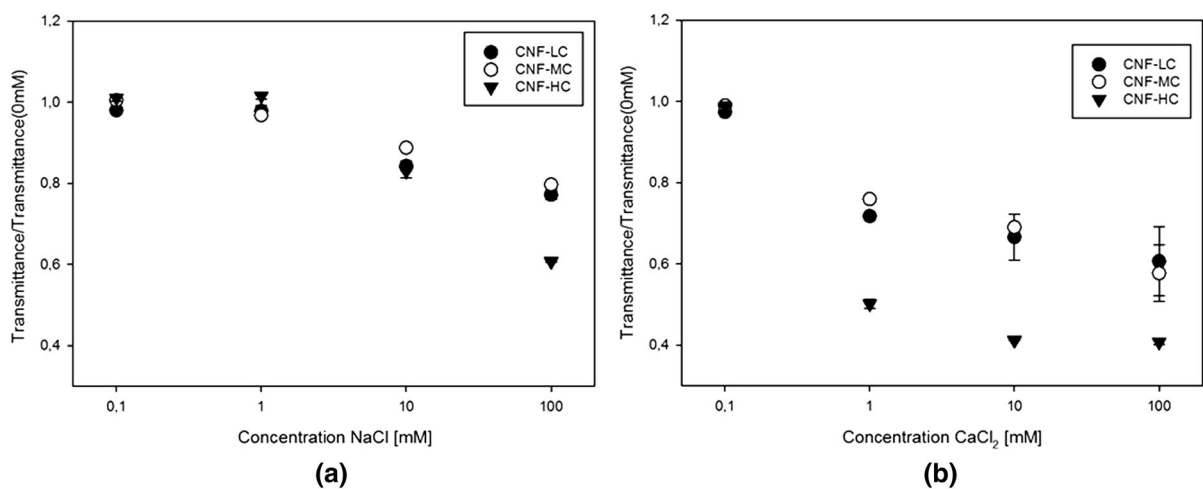


Fig. 6 The transmittance at 500 nm of salt-containing CNF samples of three different charge densities divided by the transmittance of the samples containing no electrolyte, as a

of the negative charges allows for closer contact and eventually aggregation of the fibrils. The transmittance starts to decrease at a concentration of 10 mM NaCl, with a continued decrease at 100 mM. The Schulze–Hardy rule states that the critical aggregation concentration of electrolyte correlates inversely with the sixth power of the electrolyte valence (Hardy 1900; Schulze 1882). Based on the results from NaCl addition, we can therefore expect a reduction in transmittance from about 0.16 mM of CaCl_2 . Due to a logarithmic increase in electrolyte content, this effect is first observed at 1 mM CaCl_2 . The strong screening effect of Ca^{2+} ions compared to Na^+ can be attributed to a stronger metal-carboxylate bonding for the divalent ions, causing a closer association to the fibrils, and thus more effective screening (Dong et al. 2013; Stendahl et al. 2006). The effect of the electrolytes on aggregation is especially prominent for the CNF-HC sample, where the stability caused by the highly charged fibrils is severely affected by the addition of electrolytes.

The CNF-MC sample was subjected to varying amounts of NaCl and CaCl_2 in order to study the rheological response to the electrolyte addition. Figure 7 shows the viscosity measured at 0.1 s^{-1} from the first up-curve between 0.1 and 1000 s^{-1} as a function of added NaCl or CaCl_2 .

The addition of electrolytes to a CNF dispersion will cause some screening of the negative charges on the fibril surface, leading to a lowering of the

function of the concentration of NaCl (a) and CaCl_2 (b.) Error bars representing the spreading of data are included in both figures

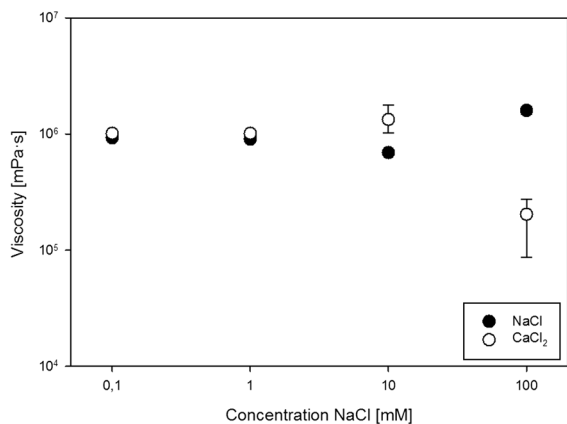


Fig. 7 The viscosity of CNF-MC samples at a shear rate of 0.1 s^{-1} from the first up-curve as a function of the concentration of NaCl and CaCl_2

electrostatic repulsion between the CNFs. For the viscosity, an initial increase could be expected as electrolyte is added, due to a stronger CNF network as the screening of charges allows for more interactions between the fibrils, and the opportunity to form more contact points between them (Aarstad et al. 2017; Dong et al. 2013). This may be the case when 10 mM CaCl_2 is added, as well as for 100 mM addition of NaCl. As observed for the transmittance, the effect of addition of electrolyte is visible at a lower concentration of CaCl_2 compared to NaCl. The large difference between the parallels after CaCl_2 -addition, apparent by large error bars, indicates a quite inhomogeneous sample, likely due to some flocculation or aggregation. As the electrolyte concentration increases, we would expect to see a drop in viscosity as the fibrils aggregate irreversibly, leaving a low-viscous layer of water around the aggregates, as described by Saarikoski et al. (2015). This is indeed observed for the sample containing 100 mM CaCl_2 , where a significant drop in viscosity was observed. This sample also contained visible aggregates.

Figure 8 shows the effect of electrolyte addition on the loss modulus and the storage modulus at 1.17 Hz and 1% strain for the CNF-MC sample.

As observed for the viscosity, an increase in both loss and storage moduli can be observed first at 10 mM CaCl_2 and 100 mM NaCl, confirming a stronger network of CNFs at these concentrations. In contrast to the viscosity measurements, a further increase to 100 mM CaCl_2 does not lead to a collapse

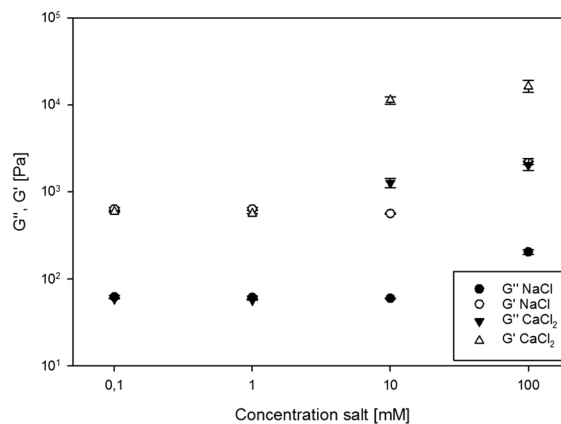


Fig. 8 The loss modulus (G'') and storage modulus (G') of the CNF-MC sample as a function of the concentration of sodium chloride and calcium chloride at 1.17 Hz and 1% strain

of the network, but rather a strengthening. This difference is not a surprising finding, as shear forces makes aggregation more likely, as shown by Saarikoski et al. (2012). The increase in moduli is also shown by Lowys et al. (2001) for concentrations of NaCl from 50 to 300 mM, and by Dong et al. (2013) for a sample of TEMPO-fibrils gelled by the addition of 50 mM $\text{Ca}(\text{NO}_3)_2$.

Higher moduli are achieved with 10 mM CaCl_2 compared to 100 mM NaCl, again emphasizing the effect of the valence of the counter-ions. Dong et al. (2013) found a correlation between primary stability constants of cations with carboxylate groups and the storage modulus of CNF gels. The stability constants, giving a measure on how closely the cations associate with carboxyl groups differs from a very low value for Na^+ (-0.07), reflecting its preference to stay in solution, to a higher value for Ca^{2+} (0.4, although not as high values as shown for the divalent transition cations (Dong et al. 2013; Stendahl et al. 2006). In our experiment the high moduli caused by Ca^{2+} compared to Na^+ is probably the result of both a more effective screening and lowering of surface charge by the more closely associated Ca^{2+} ions, and possible Ca-mediated crosslinking between fibrils.

The electrolytes present in most food systems are almost certain to affect the rheological properties of CNFs, especially if a highly charged quality is used. Using CNFs in a food system one would have to be aware of the possibility of fibril aggregation, and monitor this so the aggregates do not affect the sensory properties of the food in a negative way.

Shear forces during processing can also affect the onset of aggregation. At the same time, by using CNFs for its gel forming and structuring abilities, the presence of electrolytes can contribute to reduce the amount of CNFs needed in the system, as the moduli increase when electrolytes are added.

Effects of mixing xanthan and CNFs

The common food additive xanthan gum and CNF-MC were mixed at different ratios with either water or a 100 mM sodium chloride solution as the dispersion medium. The total concentration of xanthan and CNFs combined was 1.11 wt% for all mixtures, so that, as an example, a CNF/xanthan mixture with 0.28 wt% CNFs, contained 0.83 wt% xanthan. Samples with only CNFs or xanthan at different concentrations were also prepared for comparison. The viscosity and the storage modulus were measured using a rheometer. The viscosity of CNFs and xanthan dispersed in water and in 100 mM NaCl, at a shear rate of 0.1 s^{-1} from the first up-curve, is shown in Fig. 9 as a function of CNF and xanthan concentration.

As xanthan gum and CNFs are both negatively charged, interactions between them are not favored. It has previously been shown that negative polymers such as xanthan and CMC does not significantly adsorb onto cellulose fibers or fibrils at electrolyte-free conditions, while CMC has been shown to adsorb

unto the fibril surface when high ionic strength is applied to reduce the electrostatic repulsion (Orelma et al. 2012; Sorvari et al. 2014). Under shear, the addition of negatively charged polymers such as CMC and xanthan has been shown to better disperse a 0.5% CNF dispersion, weakening their interactions, and reducing flocculation (Myllytie et al. 2009; Sorvari et al. 2014).

As xanthan is a stiff polymer, it contributes with viscosity on its own, though as can be seen from Fig. 9a, not in the same range as the CNFs. At a low CNF/xanthan ratio, we can still assume that the contribution of viscosity given by xanthan will be notable in the mixed CNF/xanthan dispersion. On the other hand, the ability of xanthan to disturb the interactions between CNFs will work against an increase in viscosity for the CNF/xanthan mixtures. Our results (Fig. 9b) show that the viscosity of 0.28 wt% CNFs is greatly improved by the addition of 0.83 wt% xanthan, likely because of the viscosifying ability xanthan contributes with at such a high concentration. However, when the CNF/xanthan ratio increases from 0.33 to 1 or 3, the viscosity of the CNF dispersions in electrolyte-free conditions is reduced by the addition of xanthan. For these dispersions, the reduced amount of xanthan gives less potential to contribute with viscosifying abilities. At the same time, the higher CNF content allows for a more connected fibril network, which may be more

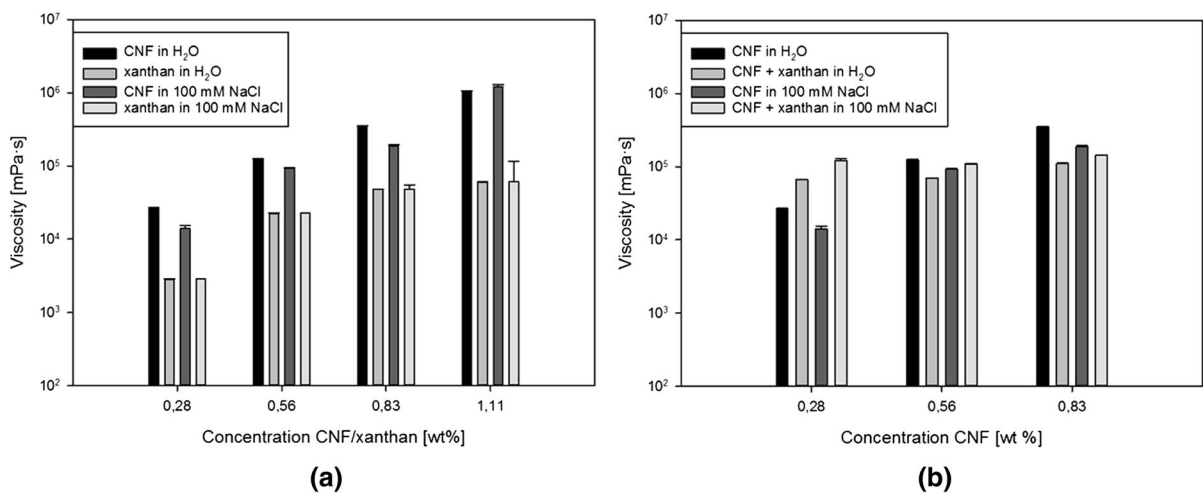


Fig. 9 The viscosity of CNF-MC and xanthan (a) and of mixtures of these two (b) dispersed in water or in 100 mM sodium chloride. In the samples containing both compounds,

the total content of xanthan and CNFs is always 1.11 wt%. The viscosity was measured at a shear rate of 0.1 s^{-1} , and the values are from the first up-curve

vulnerable to the repulsive forces introduced by the xanthan polymers.

The use of 100 mM NaCl as the dispersion medium gave a reduction in viscosity for all the CNF dispersions except for the one with 1.11 wt% CNFs, when compared to the results at electrolyte-free conditions (Fig. 9a). This may imply that the onset of breakdown of the fibril network and subsequent aggregation occurs at a lower ionic strength for dispersions with a lower CNF content. In this case, the xanthan may contribute positively to the viscosity of the mixtures, by preventing aggregates from forming. This may be the reason why the addition of 0.56 wt% xanthan to the 0.56 wt% CNF dispersion does not lead to the same drop in viscosity as seen under electrolyte-free conditions. From Fig. 9b it can also be observed that compared to the electrolyte-free conditions, the addition of xanthan leads to a greater increase in viscosity for the 0.28/0.83 CNF/xanthan dispersion, and a smaller decrease in viscosity for the 0.83/0.28 dispersion when 100 mM NaCl is used as dispersion medium.

Figure 10 shows the storage modulus at 1.17 Hz and 1% strain for increasing concentrations of CNFs and xanthan, both individually (Fig. 10a) and in mixtures (Fig. 10b), with either water or 100 mM NaCl as the dispersion medium.

Xanthan has previously been shown to lower the storage modulus for a CNF dispersion under electrolyte-free conditions (Sorvari et al. 2014). As the

modulus is dependent on the strength and number of fiber or fibril contact points, the authors explain the decrease in modulus with an ability of xanthan to disperse the CNFs more effectively and weaken their interactions (Kerekes et al. 1985; Sorvari et al. 2014). Our results, as shown in Fig. 10, rather show an increase in storage modulus as xanthan is added to the CNF dispersions. However, the relative increase gets smaller as the CNF/xanthan ratio increases. Our highest CNF/xanthan ratio is $0.83/0.28 \approx 3$, compared to a ratio of minimum $0.5/0.11 \approx 5$ in the work of Sorvari et al. (2014). The negatively charged xanthan polymers also have some ability to structure the water phase and contribute to a more gel-like behavior, but not at very low concentrations, as seen in Fig. 10a. At lower CNF concentrations, it is reasonable to assume fewer fibril contact points, and the fibrils are less constrained in their movements relative to each other, compared to in a dispersion with higher CNF concentration. As the CNF concentration increases, more fibril–fibril connections are made, and the repulsion between the fibrils themselves makes the network less flexible. When xanthan is added to one of these denser CNF networks, the strain on the fibril contact points may be too high, and cause the loss of contact points rather than stabilization of the fibril network.

In 100 mM NaCl, the storage modulus is higher for all concentrations of CNF dispersions compared to the electrolyte-free conditions. This increase is

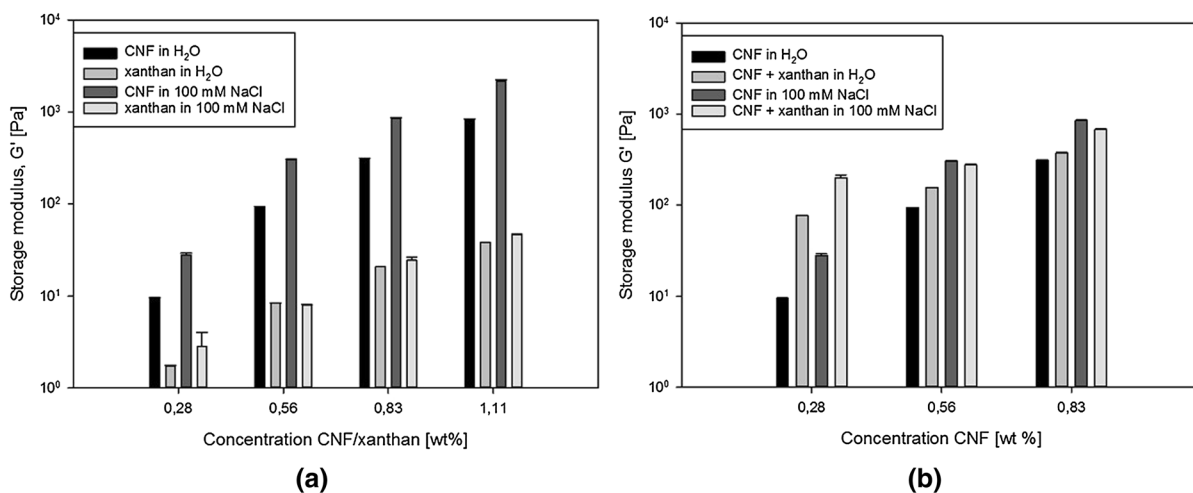


Fig. 10 The storage modulus of CNF-MC and xanthan (a) and of mixtures of these two (b) dispersed in water or 100 mM sodium chloride. In the samples containing both compounds,

the total content of xanthan and CNFs is always 1.11 wt%. The storage modulus was measured at a frequency of 1.17 Hz and 1% strain

probably due to increased strength and number of fibril contact points as the electrostatic repulsion between the fibrils are reduced by the sodium ions. Under these conditions, with more connected fibril networks, 0.28 wt% CNFs is the only CNF dispersion benefiting from addition of xanthan. For the other two CNF dispersions, a slight decrease in storage modulus can be observed with the addition of xanthan.

From these results, it seems that the ratio between added CNFs and other components in the food systems is an extremely important factor, as a changing ratio can lead to great changes in their interaction and rheological behavior.

Conclusions

The rheological response of TEMPO-oxidized CNF dispersions to concentration, addition of electrolytes and xanthan has been evaluated to assess the suitability of CNFs as fat replacers in low-fat food products. The CNF dispersions were shear thinning across the concentration range, and showed gel-like behavior, as have previously been observed by other groups for CNF dispersions (Iotti et al. 2011; Lasseguette et al. 2008; Naderi et al. 2014b; Pääkkö et al. 2007). The dependency of viscosity and storage modulus on CNF concentration followed a power law, with exponents 2.6–3.3 for the viscosity and 3.6 for the storage modulus. Decreasing transmittance for CNF dispersions as electrolytes are added indicates a change in flocculation or aggregation from 10 mM NaCl, or 1 mM CaCl₂, which is also reflected in the rheological measurements where electrolytes are present. As to other food components, we have found that the effect of xanthan addition to the rheology of CNF dispersions seems to be extremely dependent on the ratio between the two components. At low CNF/xanthan ratios, the viscosifying and structuring abilities of xanthan contribute to increase both the viscosity and the storage modulus for CNF-dispersions. As the CNF/xanthan ratio or the concentration of CNF increases, the weakening of connections described by Sorvari et al. (2014) seems to counter the positive contribution from xanthan, shown by a reduction in viscosity and a lower increase in storage modulus. With 100 mM NaCl present, the CNF network is strengthened, and a reduction in storage modulus can be observed when xanthan is added to

the dispersion with the highest CNF concentration. For the viscosity, the ionic strength introduced by 100 mM NaCl leads to aggregation of the fibrils, and xanthan can probably counter this to some extent by keeping the fibrils better dispersed.

Based on these findings we believe that CNFs can contribute with elevated viscosity and modulus as fat replacers in foodstuff, even at low concentrations. The salt content in food can contribute to reduce the required amount of CNFs needed to obtain a desired storage modulus even further. The highly charged CNF qualities may be less suited for foods with a high salt content, especially if the food product is subjected to high shear during processing, as this can induce aggregation of the fibrils. Other food components, such as xanthan, can affect the amount of electrolyte tolerated by the dispersed CNFs. We have also found that not only the CNF concentration, but also the ratio between CNFs and other food additives such as xanthan, can greatly affect the rheological properties of CNF systems. For this reason, the amount of CNFs needed to acquire the desired rheological properties in a food system will be very dependent on the existing composition of the individual system. To get a better understanding of the potential of CNFs as fat replacers, future work should include work on specific food systems or model systems where more ingredients are present.

Acknowledgments This work has been partly funded by the Research Council of Norway through the NANO2021 Project NanoVisc, (Grant No. 245300), initiated and led by RISE PFI, and partly funded by the companies Borregaard, Stora Enso, Mercer and the foundation Papirindustriens Forskningsinstitutt. The authors would like to thank Per Olav Johnsen and Birgitte Hjelmeland McDonagh (RISE PFI) for their excellent laboratory assistance.

References

- Aarstad O, Heggset EB, Pedersen IS, Bjørnøy SH, Syverud K, Strand BL (2017) Mechanical properties of composite hydrogels of alginate and cellulose nanofibrils. *Polymers* 9:378
- Agoda-Tandjawa G, Durand S, Berot S, Blassel C, Gaillard C, Garnier C, Doublier J-L (2010) Rheological characterization of microfibrillated cellulose suspensions after freezing. *Carbohydr Polym* 80:677–686
- Barnes HA (1995) A review of the slip (wall depletion) of polymer solutions, emulsions and particle suspensions in viscometers: its cause, character, and cure. *J Non-newton*

- Fluid Mech 56:221–251. [https://doi.org/10.1016/0377-0257\(94\)01282-M](https://doi.org/10.1016/0377-0257(94)01282-M)
- Buscall R, McGowan JJ, Morton-Jones AJ (1993) The rheology of concentrated dispersions of weakly attracting colloidal particles with and without wall slip. *J Rheol* 37:621–641
- Chen W, Yu H, Liu Y (2011) Preparation of millimeter-long cellulose I nanofibers with diameters of 30–80 nm from bamboo fibers. *Carbohydr Polym* 86:453–461. <https://doi.org/10.1016/j.carbpol.2011.04.061>
- Cheung I, Gomes F, Ramsden R, Roberts D (2002) Evaluation of fat replacers Avicel™, N Lite S™ and Simplesse™ in mayonnaise. *Int J Consumer Stud* 26:27–33
- Cousins SK, Brown RM (1997) X-ray diffraction and ultrastructural analyses of dye-altered celluloses support van der Waals forces as the initial step in cellulose crystallization. *Polymer* 38:897–902
- Derjaguin B, Landau L (1941) The theory of stability of highly charged lyophobic sols and coalescence of highly charged particles in electrolyte solutions. *Acta Physicochim URSS* 14:58
- Dong H, Snyder JF, Williams KS, Andzelm JW (2013) Cation-induced hydrogels of cellulose nanofibrils with tunable moduli. *Biomacromolecules* 14:3338–3345
- Fall AB, Lindström SB, Sundman O, Ödberg L, Wågberg L (2011) Colloidal stability of aqueous nanofibrillated cellulose dispersions. *Langmuir* 27:11332–11338
- Food Standards Agency (2010) Eat well-your guide to healthy eating. Accessed 1 Nov 2017
- Fukuzumi H, Tanaka R, Saito T, Isogai A (2014) Dispersion stability and aggregation behavior of TEMPO-oxidized cellulose nanofibrils in water as a function of salt addition. *Cellulose* 21:1553–1559. <https://doi.org/10.1007/s10570-014-0180-z>
- Gardner K, Blackwell J (1974) The structure of native cellulose. *Biopolymers* 13:1975–2001
- González-Tomás L, Bayarri S, Taylor A, Costell E (2007) Flavour release and perception from model dairy custards. *Food Res Int* 40:520–528
- Hardy WB (1900) A preliminary investigation of the conditions which determine the stability of irreversible hydrosols. *J PhysChem* 4:235–253
- Heggset EB, Chinga-Carrasco G, Syverud K (2017) Temperature stability of nanocellulose dispersions. *Carbohydr Polym* 157:114–121
- Heggset EB, Strand BL, Sundby KW, Simon S, Chinga-Carrasco G, Syverud K (2019) Viscoelastic properties of nanocellulose based inks for 3D printing and mechanical properties of CNF/alginate biocomposite gels. *Cellulose* 26:581–595
- Herrick FW, Casebier RL, Hamilton JK, Sandberg KR (1983) Microfibrillated cellulose: morphology and accessibility. *J Appl Polym Sci Appl Polym Symp* 37:797–813
- Heyn AN (1969) The elementary fibril and supermolecular structure of cellulose in soft wood fiber. *J Ultrastruct Res* 26:52–68
- Iotti M, Gregersen ØW, Moe S, Lenes M (2011) Rheological studies of microfibrillar cellulose water dispersions. *J Polym Environ* 19:137–145
- Isomaa B et al (2001) Cardiovascular morbidity and mortality associated with the metabolic syndrome. *Diabetes Care* 24:683–689
- James PT, Rigby N, Leach R (2004) The obesity epidemic, metabolic syndrome and future prevention strategies. *Eur J Cardiovasc Prev Rehabil* 11:3–8
- Jellema RH, Janssen AM, Terpstra ME, de Wijk RA, Smilde AK (2005) Relating the sensory sensation ‘creamy mouthfeel’ in custards to rheological measurements. *J Chemom* 19:191–200
- Jowkarderis L, van de Ven TGM (2015) Rheology of semi-dilute suspensions of carboxylated cellulose nanofibrils. *Carbohydr Polym* 123:416–423
- Kerekes R, Soszynski R, Tam Doo P (1985) The flocculation of pulp fibres. *Papermak Raw Mater* 1:265
- Lasseguette E, Roux D, Nishiyama Y (2008) Rheological properties of microfibrillar suspension of TEMPO-oxidized pulp. *Cellulose* 15:425–433. <https://doi.org/10.1007/s10570-007-9184-2>
- Lowys M-P, Desbrieres J, Rinaudo M (2001) Rheological characterization of cellulosic microfibril suspensions. Role of polymeric additives. *Food Hydrocoll* 15:25–32
- Lucca PA, Tepper BJ (1994) Fat replacers and the functionality of fat in foods. *Trends Food Sci Technol* 5:12–19
- Mudgil D, Barak S (2013) Composition, properties and health benefits of indigestible carbohydrate polymers as dietary fiber: a review. *Int J Biol Macromol* 61:1–6
- Myllytie P, Holappa S, Paltakari J, Laine J (2009) Effect of polymers on aggregation of cellulose fibrils and its implication on strength development in wet paper web. *Nord Pulp Pap Res J* 24:125–134
- Naderi A, Lindström T (2014) Carboxymethylated nanofibrillated cellulose: effect of monovalent electrolytes on the rheological properties. *Cellulose* 21:3507–3514. <https://doi.org/10.1007/s10570-014-0394-0>
- Naderi A, Lindström T, Pettersson T (2014a) The state of carboxymethylated nanofibrils after homogenization-aided dilution from concentrated suspensions: a rheological perspective. *Cellulose* 21:2357–2368. <https://doi.org/10.1007/s10570-014-0329-9>
- Naderi A, Lindström T, Sundström J (2014b) Carboxymethylated nanofibrillated cellulose: rheological studies. *Cellulose* 21:1561–1571
- Nechyporchuk O, Belgacem MN, Pignon F (2014) Rheological properties of micro-/nanofibrillated cellulose suspensions: wall-slip and shear banding phenomena. *Carbohydr Polym* 112:432–439. <https://doi.org/10.1016/j.carbpol.2014.05.092>
- Orelma H, Teerinen T, Johansson L-S, Holappa S, Laine J (2012) CMC-modified cellulose biointerface for antibody conjugation. *Biomacromolecules* 13:1051–1058. <https://doi.org/10.1021/bm201771m>
- Pääkkö M et al (2007) Enzymatic hydrolysis combined with mechanical shearing and high-pressure homogenization for nanoscale cellulose fibrils and strong gels. *Biomacromolecules* 8:1934–1941
- Payen A (1838) Sur un Moyen d’isoler le Tissu Élémentaire des Bois. *C R Hebd des Seances de l’Acad des Sci* 7:1125
- Purves C (1954) Chain structure in cellulose and cellulose derivatives: part I. Wiley, New York
- Roller S, Jones SA (1996) Handbook of fat replacers. CRC Press, Boca Raton
- Saarikoski E, Saarinen T, Salmela J, Seppälä J (2012) Flocculated flow of microfibrillated cellulose water

- suspensions: an imaging approach for characterisation of rheological behaviour. *Cellulose* 19:647–659
- Saarikoski E, Rissanen M, Seppälä J (2015) Effect of rheological properties of dissolved cellulose/microfibrillated cellulose blend suspensions on film forming. *Carbohydr Polym* 119:62–70
- Saito T, Isogai A (2004) TEMPO-mediated oxidation of native cellulose. The effect of oxidation conditions on chemical and crystal structures of the water-insoluble fractions. *Biomacromolecules* 5:1983–1989. <https://doi.org/10.1021/bm0497769>
- Saito T, Isogai A (2006) Introduction of aldehyde groups on surfaces of native cellulose fibers by TEMPO-mediated oxidation. *Colloids Surf Physicochem Eng Asp* 289:219–225. <https://doi.org/10.1016/j.colsurfa.2006.04.038>
- Saito T, Nishiyama Y, Putaux J-L, Vignon M, Isogai A (2006) Homogeneous suspensions of individualized microfibrils from TEMPO-catalyzed oxidation of native cellulose. *Biomacromolecules* 7:1687–1691
- Saito T, Kimura S, Nishiyama Y, Isogai A (2007) Cellulose nanofibers prepared by TEMPO-mediated oxidation of native cellulose. *Biomacromolecules* 8:2485–2491
- Sandoval-Castilla O, Lobato-Calleros C, Aguirre-Mandujano E, Vernon-Carter E (2004) Microstructure and texture of yogurt as influenced by fat replacers. *Int Dairy J* 14:151–159
- Saxena IM, Brown RM Jr (2005) Cellulose biosynthesis: current views and evolving concepts. *Ann Bot* 96:9–21
- Schulze H (1882) Schwefelarsen in wässriger Lösung. *J für praktische Chemie* 25:431–452
- Sorvari A, Saarinen T, Haavisto S, Salmela J, Vuoriluoto M, Seppälä J (2014) Modifying the flocculation of microfibrillated cellulose suspensions by soluble polysaccharides under conditions unfavorable to adsorption. *Carbohydr Polym* 106:283–292. <https://doi.org/10.1016/j.carbpol.2014.02.032>
- Stendahl JC, Rao MS, Guler MO, Stupp SI (2006) Inter-molecular forces in the self-assembly of peptide amphiphile nanofibers. *Adv Funct Mater* 16:499–508
- Tatsumi D, Ishioka S, Matsumoto T (2002) Effect of fiber concentration and axial ratio on the rheological properties of cellulose fiber suspensions. *日本レオロジー学会誌* 30:27–32
- Torres IC, Janhøj T, Mikkelsen BØ, Ipsen R (2011) Effect of microparticulated whey protein with varying content of denatured protein on the rheological and sensory characteristics of low-fat yoghurt. *Int Dairy J* 21:645–655
- Turbak AF, Snyder FW, Sandberg KR (1983). Microfibrillated cellulose. Google Patents
- U.S. Department of Health and Human Services and U.S. Department of Agriculture (2015) 2015–2020 dietary guidelines for Americans, 8th edn. <http://health.gov/dietaryguidelines/2015/guidelines/>. Accessed 8 Dec 2016
- USDA (2018) USDA food composition databases, vol 2018. USDA. <https://ndb.nal.usda.gov/ndb/search/list?home=true>. Accessed 18 Oct 2018
- Van Gaal LF, Mertens IL, Christophe E (2006) Mechanisms linking obesity with cardiovascular disease. *Nature* 444:875–880
- Verwey J, Overbeek T (1948) Theory of the stability of lyophobic colloids. *Advances in colloid interface science*. Elsevier, Amsterdam

Publisher's Note Springer Nature remains neutral with regard to jurisdictional claims in published maps and institutional affiliations.